SURVEYING THE SOUTH POLE-AITKEN BASIN MAGNETIC ANOMALY FOR REMNANT IMPACTOR METALLIC IRON.

J.T.S. Cahill[1], D.J. Lawrence[1], J.J. Hagerty[2], R.L. Klima[1], and D.T. Blewett[1]. [1]Johns Hopkins Applied Physics Laboratory, Laurel, MD (Joshua.Cahill@jhuapl.edu), [2]U. S. Geological Survey, Astrogeology Science Center, Flagstaff, AZ.

Introduction: For several decades it has been known that portions of the lunar crust are strongly magnetized [1-4]; yet the origin of this magnetization is yet to be fully understood. Difficulties discerning a source for these anomalies begin with most of them having no consistent association with known geologic structures. Impact basins, impact basin ejecta, and antipodes are some of the few geologic structures that readily associate with a minority of magnetic anomalies [5], but most of these show weak magnetization relative to the globally observed dynamic range. Further, there are many of these same structures that do not show magnetic anomalies. It is difficult to reconcile the strengths of many of these anomalies with lunar samples, as most lunar materials (i.e., silicates) are very weakly magnetic relative to terrestrial materials. Measurements of mare basalt and pristine highlands rock magnetization show that they are substantially weaker than mid-ocean ridge basalts (2-4 orders of magnitude) [6]. An additional complication is that the lithologies that comprise lunar magnetic anomalies are not rigorously constrained. As a result, it is difficult to discern if the magnetization of materials in these anomalies is derived from crystallization or from impact shock [7, 8].

Recently, Wieczorek et al. [9] presented a study suggesting that a unique cluster of magnetic anomalies on the southern farside of the Moon is attributable to remnant metallic iron from the impactor that created South Pole-Aitken basin (SPA) [9]. In that study, Wieczorek et al. [9] argued that the distribution of projectile materials roughly coincided with the distribution of magnetic anomalies near the northern rim of SPA. Wieczorek et al. [9] noted that typical chondritic projectile materials are approximately two times more magnetic than average lunar crustal materials. If the SPA-forming projectile were similar to an undifferentiated chondrite, then the thickness of the ejecta needed to account for the magnetism of materials north of SPA would only need to be a few hundred meters thick. The thickness would be possibly less if the projectile were differentiated into core, mantle, and crustal components. Here we begin to evaluate this hypothesis by considering if an excess of iron can be detected in remote-sensing data sets.

Method: The presence of metallic iron is difficult to quantify using near infrared (NIR) reflectance spectroscopy for several reasons. In general, metallic iron is relatively featureless in the NIR, with no prominent absorption features that could reveal its presence in a surficial mixture. Furthermore, metallic iron is one of the mineral species, along with ilmenite, unlikely to be directly accounted for in NIR iron-determination methods [10-15] due to the positioning of the wavelength bands employed by these algorithms. To complicate matters further, metallic iron is generally present only in very small proportions (<1 wt. %) in lunar samples. Despite these factors, metallic iron has a substantial influence on NIR spectra by reddening and darkening spectra in ways that are dependent upon grain size [16]. In contrast, gamma-ray spectroscopy is useful for absolute determination of iron, but is unable to differentiate the mineral species in which iron may occur. Here we exploit a combination of NIR and gamma-ray spectroscopy in an attempt to detect the presence of metallic iron (or lack thereof).

While most analysis methods applied to Clementine spectral reflectance (CSR) derived FeO abundances show reasonable agreement both to each other and the Lunar Prospector Gamma-ray Spectrometer (GRS) derived FeO abundances, important differences (±6 wt.%) remain for various locales on the Moon (**Fig. 1**) [14]. In some cases, these discrepancies are large enough to suggest different plausible interpretations regarding surface composition and history. Here we examine differences between CSR- and GRS-determined iron content to evaluate whether metallic iron could be a constituent in the magnetic anomalies circumferential to SPA. The assumption is that the presence of metallic iron should be detected by GRS, but would not be detectable by CSR algorithms. Excess metallic iron would produce a positive δFeO ($FeO_{GRS} - FeO_{CSR}$). If unusual amounts of metallic iron are not present, δFeO would be zero or negative.

Results: Comparison of δFeO and magnetic mapping products show that magnetic anomalies exist in both areas where GRS estimates are higher and in areas where CSR estimates are higher. As a result, the spatial positioning of GRS and CSR disagreements do not fully support or refute the iron-bearing-impactor hypothesis. It can be argued that the higher GRS FeO estimates and the magnetic anomalies outside the rim

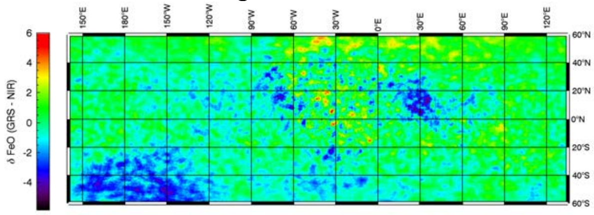

Figure 1: *Difference (δFeO) in lunar surface FeO as observed by Lunar Prospector and Clementine.*

of SPA are consistent with the presence of additional metallic iron (**Fig. 2**). However, there are several factors that prevent a straightforward interpretation. First, neither the spatial locations of the strongest magnetic anomalies, nor their dynamic range in intensity appear to correlate with the magnitude of δFeO. Second, in the magnetically quiet northern farside highlands, δFeO values fluctuate in a manner similar to those within the cluster of magnetic anomalies. A magnetic anomaly is also observed within the northeastern portion of the SPA basin. The deviation in FeO here (negative) is attributed to higher than normal orthopyroxene abundances that bias the CSR algorithm toward lower than actual FeO [14]. In this case, if additional meteoritic metallic iron is present, its signature in our δFeO maps could be offset by very high abundances of orthopyroxene.

Conclusions: Here we combined LP-GRS and CSR FeO products in an effort to evaluate the hypothesis of [9] that remnant metallic iron produced the magnetic anomaly observed dominantly outside the northern rim of SPA. Our results are ultimately inconclusive regarding enrichment in metallic iron in this region. Delta FeO is indeed higher north of SPA as observed by GRS and might suggest detection of remnant metallic iron. However, excess GRS FeO is found evenly distributed through out the farside highlands. The remnant high-Fe materials would have had to have covered the farside highlands in ejecta, and then avoid being covered with a subsequent 10 cm of regolith due to billions of subsequent years of impact processes. Furthermore, δFeO and magnetic anomalies are not spatially correlated or do not show corresponding dynamic intensity ranges.

Ultimately, due to the old age of SPA and subsequent impact mixing, it is plausible that the materials responsible for the magnetic anomaly are now too deep to be detected by either optical or gamma-ray observations. For example, the origin of the strong magnetic anomaly at Reiner Gamma apparently lies beneath the basalts of Oceanus Procellarum [17].

Acknowledgments: NASA supported this work through LASER Program grant NNH09AL71I.

References: [1] Dyal et al. (1974) RGSP, 12, 568. [2] Hood et al. (2001) JGR, 106, 27,825. [3] Mitchell et al. (2008) Icarus, 194, 401. [4] Purucker and Nicholas (2010) JGR, 115. [5] Richmond et al. (2005) JGR, 110, E05011. [6] Wang et al. (2005) Geosphere, 1, 138. [7] Fuller and Cisowski, in *Geomagnetism*, Jacobs, Ed. 1987, 307. [8] Gattacceca (2010) EPSL, 299. [9] Wieczorek et al. (2012) Science, 335, 1212. [10] Lucey et al. (2000) JGR, 105, 20,297. [11] Le Mouélic et al. (2000) JGR, 105, 9445. [12] Fischer and Pieters (1994) Icarus, 111, 475-488. [13] Wilcox et al. (2005) JGR, 110. [14] Lawrence et al. (2002) JGR, 107, 5130. [15] Blewett et al. (1997) JGR, 102, 16319. [16] Lucey and Riner (2011) Icarus, 212, 451. [17] Nicholas et al. (2007) GRL, 34, L02205.

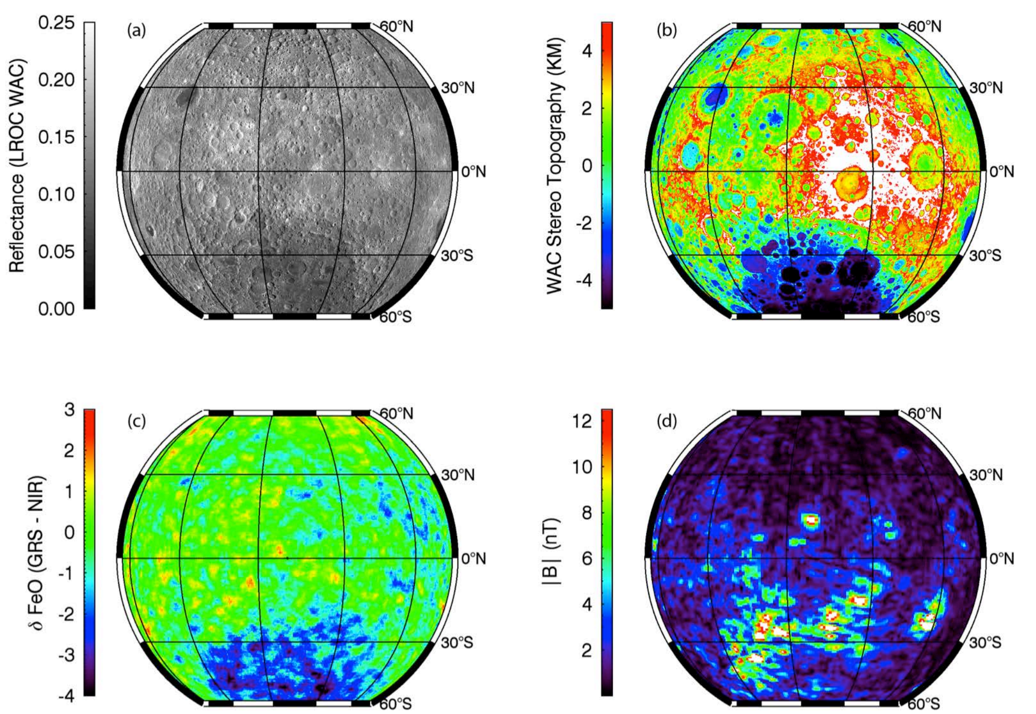

Figure 2: Observations of the farside of the Moon via (a and b) LROC optical and stereo topography, (c) δFeO, and (d) Lunar Prospector magnetic data of [4].